Heat Mass Transfer (2016) 52:805–817
DOI 10.1007/s00231-015-1602-7

ORIGINAL

Solution of boundary heat transfer coefficients between hot stamping die and cooling water based on FEM and optimization method

Huiping Li[1] · Lianfang He[1] · Chunzhi Zhang[1] · Hongzhi Cui[1]

Received: 8 September 2014 / Accepted: 30 May 2015 / Published online: 6 June 2015

Abstract The thermal physical parameters have significant effects on the calculation accuracy of physical fields, and the boundary heat transfer coefficient between the die and water is one of the most important thermal physical parameters in the hot stamping. In order to attain the boundary heat transfer coefficient, the testing devices and test procedures are designed according to the characteristic of heat transfer in the hot stamping die. A method of estimating the temperature-dependent boundary heat transfer coefficient is presented, and an inverse heat conduction software is developed based on finite element method, advance-retreat method and golden section method. The software is used to calculate the boundary heat transfer coefficient according to the temperatures measured by NiCr–NiSi thermocouples in the experiment. The research results show that, the convergence of the method given in the paper is well, the surface temperature of sample has a significant effect on the boundary heat transfer coefficient between the die and water. The boundary heat transfer coefficient increases as the surface temperature of sample reduces, and the variation is nonlinear.

List of symbols

k	Thermal conductivity
T	Temperature
q_v	Latent heat of phase-transformation
ρ	Density
c_p	Constant pressure specific heat
t	Time
x, y and z	Cartesian coordinates
n	Outer normal of boundary surface
H_k	Convection coefficient
H_s	Radiation coefficient
T_w	Temperature of boundary
T_c	Temperature of ambience
H	Boundary heat transfer coefficient (BHTC)
$E(x)$	Function of standard deviation
f	Absolute value of $E(x)$
m	Total number of target points
T_i	Temperature of ith target point measured by sensor
$\hat{T}_i$	Temperature of ith target point evaluated by numerical simulation
α	Step size of searching the interval
$E(a)$	Value relative to the left end-point of interval $[a, b]$
$E(b)$	Value relative to the right end-point of interval $[a, b]$

1 Introduction

In order to reduce the spring-back and forming force of ultra high strength steels, hot stamping was presented in recent years, and some researchers have been studying the numerical simulation of hot stamping. In the simulation of hot stamping, the thermal physical parameters have significant effects on the calculation accuracy of physical fields, and the boundary heat transfer coefficient (BHTC) in the hot stamping is one of the most important thermal physical parameters. The solution of BHTC is one of the inverse heat conduction problems (IHCP). It is an ill-posed problem and more difficult to solve than the normal heat exchange problem. For IHCP, some sensors laid at some

✉ Huiping Li
lihuiping99@163.com

[1] School of Materials Science and Engineering, Shandong University of Science and Technology, 579 Qianwangang Road, Qingdao 266590, Shandong, People's Republic of China

certain positions should be used to record the temperatures of part. The unknown conditions, such as BHTC and boundary temperature, can be reckoned by some special methods according to the temperature variation.

Many researchers have studied the solution of IHCP, and presented some useful methods. According to the temperature–time data of several interior locations in the quenching part measured by sensors, Gu et al. [1] used the inverse heat conduction method to estimate the heat transfer coefficients between quenching part and water or oil. Based on the Karhunen–Loeve Galerkin procedure, Park et al. [2] presented a method for the solution of inverse heat conduction problems of estimating the time-varying strength of a heat source in a two-dimensional heat conduction system. Taler and Zima [3] used the control volume method to solve multi-dimensional inverse heat conduction problems. Chantasiriwan [4] studied the one-dimensional problem of estimating the transient heat transfer coefficient at the surface of steel bars using the sequential function specification method. Chen et al. [5] estimated the heat transfer coefficients between quenching part and quenching medium using the inverse heat conduction method. Li et al. [6] calculated the temperature-dependent BHTC in the quenching, and the phase-transformation latent heat is considered to improve the calculation precision of temperature. Moreover, Lesnic, Kim, Taler, Shen and Tseng respectively presented the boundary element method [7], decomposition method [8], integral method [9], Tikhonov's regularization method [10], direct sensitivity coefficient method [11] to solve the inverse heat conduction problems.

In the hot stamping, there are two types of BHTC, one is the BHTC between the boron steel plate and hot stamping tools, and the other is the BHTC between the flowing water and hot stamping tools. Hot stamping can be used to produce the components with distributed microstructure and mechanical properties by using the slow cooling rate for the special region in hot stamping [12]. Local reductions of cooling rate can be achieved by using the thin air gap between the tools and the blank [13], controlling the temperature of tools [14], or using the steel with the lower thermal conductivity in the tools [15]. The production of structural parts with distributed mechanical properties requires a precise control of the local cooling rate and temperature of tools [16]. This can only be achieved with an accurate knowledge of the two type of BHTC in the hot stamping.

Some researchers have studied the BHTC between the boron steel plate and tools. Bosetti et al. [17] calculated the BHTC between the steel sheets and tools under conditions very close to the industrial ones. Abdulhay et al. [18, 19] designed an experimental device to accurately measure the thermal contact resistance under representative process conditions, and presented an approach to determine the evolution of the thermal contact resistance under different contact pressure (2–30 MPa). The research results of Li et al. [20] show that, the oxidation of boron steel has a remarkable effect on the surface heat transfer coefficient, the surface heat transfer coefficient increases with the rise of boundary pressure, and the relationship is approximately linear. All above research results show the BHTC between the boron steel plate and tools depends on the pressure. Some other research results show the BHTC between the boron steel plate and tools also depends on boundary temperature difference [21].

In this paper, the BHTC between the flowing water and tools is researched. A method of estimating the BHTC is presented, and an inverse heat conduction software is developed based on finite element method, advance-retreat method and golden section method. The software is used to calculate the BHTC according to the temperatures measured by NiCr–NiSi thermocouples in the experiment.

2 FEM model of temperature field

2.1 Basic equation

According to Fourier law, the Fourier heat conduction equation of transient problem with the phase-transformation latent heat can be achieved by using conservation of energy in a Cartesian coordinates system. The equation can be written as

$$\frac{\partial}{\partial x}\left(k\frac{\partial T}{\partial x}\right)+\frac{\partial}{\partial y}\left(k\frac{\partial T}{\partial y}\right)+\frac{\partial}{\partial z}\left(k\frac{\partial T}{\partial z}\right)+q_{\mathrm{v}}=\rho c_p\frac{\partial T}{\partial t} \quad (1)$$

where k is the thermal conductivity, T is the temperature of quenched part, q_{v} is the latent heat of phase-transformation, ρ is the density of material, c_p is the constant pressure specific heat, t is time, x, y and z are the Cartesian coordinates.

2.2 Initial condition

Initial condition is the initial temperature of quenched part. It is the starting point for calculation. The initial condition at time $t = 0$ can be described as

$$T|_{t=0} = T_0(x, y, z) \quad (2)$$

where $T_0(x, y, z)$ is the initial temperature function.

2.3 Boundary condition

Boundary condition is the way of heat exchange between quenched part and ambience. The boundary condition of quenching process is the third-type condition, and it is the mixed heat exchange boundary of convection and radiation. It can be written as

$$-k\left.\frac{\partial T}{\partial n}\right|_{\Gamma} = H_{\mathrm{k}}(T_{\mathrm{w}}-T_{\mathrm{c}})+H_{\mathrm{s}}(T_{\mathrm{w}}^4-T_{\mathrm{c}}^4)=H(T_{\mathrm{w}}-T_{\mathrm{c}}) \quad (3)$$

where n is the outer normal of boundary surface, H_k is the convection coefficient, H_s is the radiation coefficient, T_w is the temperature of boundary, T_c is the temperature of ambience. H is the BHTC, which will be calculated according to the temperatures measured in the experiment.

In the calculation of temperature, the Crank-Nicolson method [22] is used in the time domain, and FEM is used in the space domain.

3 Calculation methods

3.1 Criteria of convergence

In the solution of BHTC, the finite element method and finite difference method are used to calculate the temperature of sample. The optimization method is used to search and narrow the range of interval in which the extremum is known to exist, and finally attains the BHTC. In order to ensure the precision of calculation, it is necessary to construct a convergence criterion or optimization model. According to the characteristic of evaluating the temperature-dependent BHTC in the hot stamping, the criterion of convergence is constructed using the temperature T measured by sensor and the temperature $\hat{T}$ evaluated by numerical simulation. The criterion of convergence can be described as

$$E(x) = \begin{cases} \left(\sum_{i=1}^{m} \sqrt{(T_i - \hat{T}_i)^2}\right)/m & \left(\sum_{i=1}^{m} T_i - \sum_{i=1}^{m} \hat{T}_i \geq 0\right) \\ -\left(\sum_{i=1}^{m} \sqrt{(T_i - \hat{T}_i)^2}\right)/m & \left(\sum_{i=1}^{m} T_i - \sum_{i=1}^{m} \hat{T}_i < 0\right) \end{cases} \tag{4}$$

$$f = |E(x)| \leq \delta \tag{5}$$

where, $E(x)$ is the function of standard deviation. f is the absolute value of $E(x)$. δ is the condition of convergence, which is a very small number. m is the total number of target points. T_i is the temperature of ith target point measured by sensor. $\hat{T}_i$ is the temperature of ith target point evaluated by numerical simulation. When the value of f is not more than δ, the BHTC relative to the corresponding surface temperature can be attained.

3.2 Finding an interval

The advance-retreat method is one of one dimension searching methods in the optimization, which can be used to finding the extremum (minimum or maximum) of a strictly unimodal function. The principle of this method can be described as follows: search the interval from certain initial point along one direction, until find three points which function values show "up-down-up" trend according to certain searching step size; if it is not successful along this direction, then retreat the starting point and search the interval along other direction (along an inverse direction), as shown in Fig. 1.

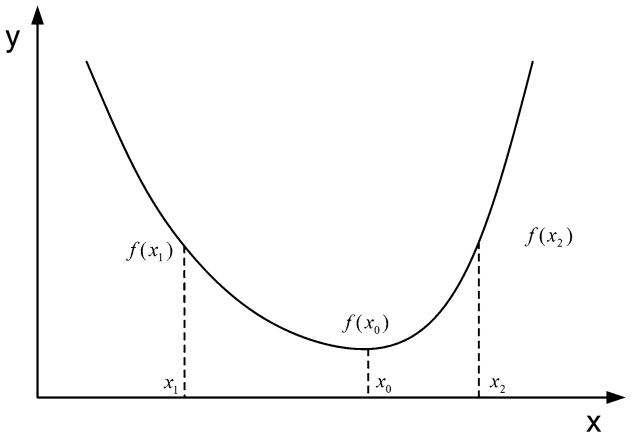

Fig. 1 Schematic diagram of advance-retreat method

In the paper, the advance-retreat method is used to find an interval, the function value of left end-point of interval is positive (more than 0), and the function value of right end-point is negative (less than 0). In the process of searching the interval by the advance-retreat method, as soon as the end-point is ascertained, the value of this point will be regard as the BHTC and be used to evaluate the temperatures in the simulation program. The time of searching an appropriate interval strongly depends on the value of initial step size α. If α is bigger, the optimization iterative time of the gold section method is increased largely although the searching time of finding the interval is decreased. If α is smaller, the time of searching an appropriate interval is increased largely although the optimization iterative time of the gold section method is decreased. In order to decrease the searching time of interval when the initial step size α keeps the same value, the advance-retreat method is improved.

There are several iterations in each time step. The values of $\hat{T}_i$ will vary with the BHTC in each iteration, and the error values relative to the different BHTC can be calculated by Eqs. 4 and 5. There is only one appropriate BHTC, which will let the error $E(x)$ enough small, and this BHTC is the objective to be found. Except this appropriate BHTC, the error $E(x)$ relative to other BHTCs will be a negative or positive number. The important step of searching the appropriate BHTC is to ascertain an interval, one endpoint of the interval can make the error $E(x)$ to be a negative number, and other endpoint of the interval can make the error $E(x)$ to be a positive number. For every BHTC, the software, which is developed by authors based on both finite element method and finite difference method, will be used to calculate $\hat{T}_i$, and then the error $E(x)$ will be calculated by Eq. 4. The flow chart of improved advance-retreat method is shown in Fig. 2.

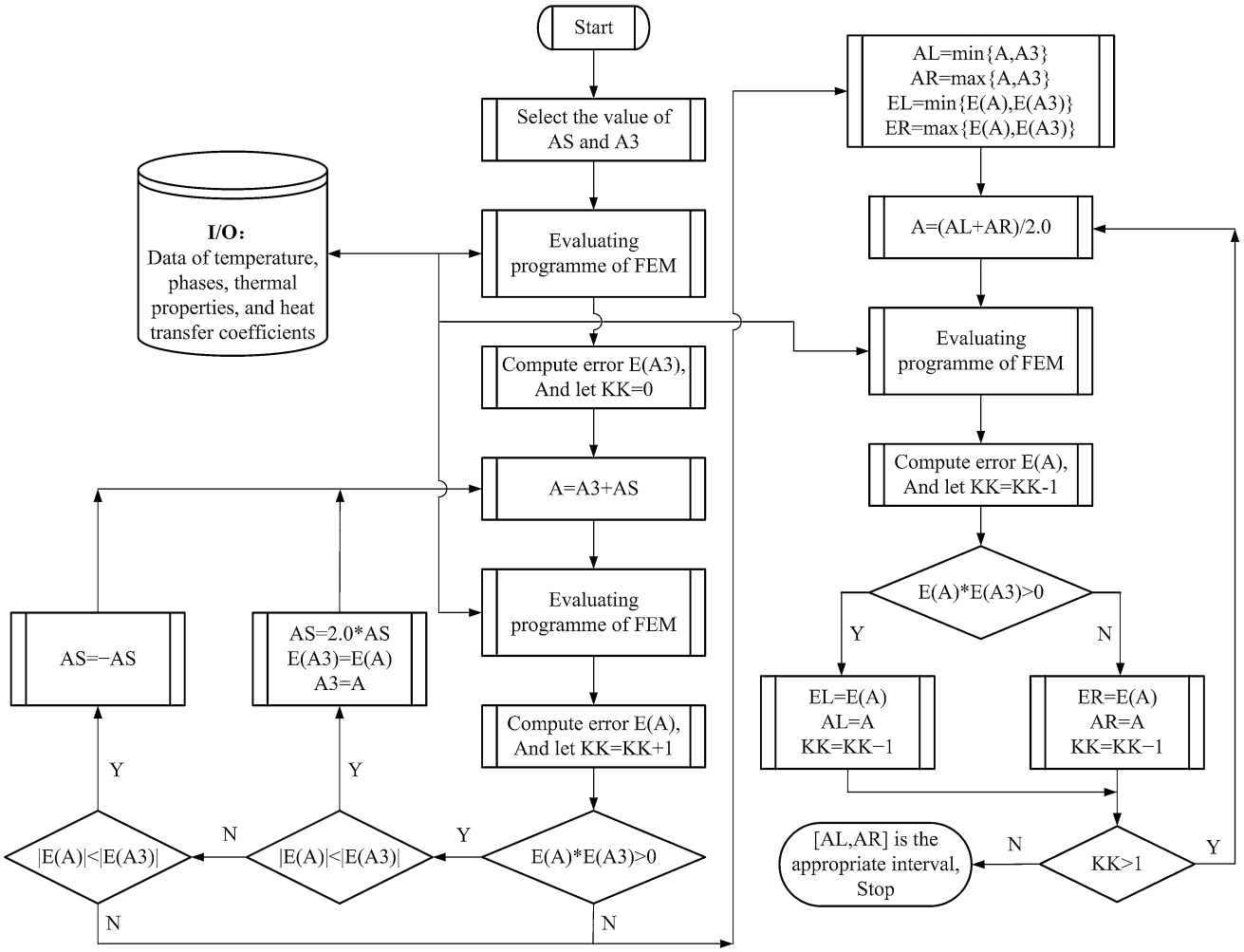

Fig. 2 Flow chart of improved advance-retreat method

In order to find the appropriate interval, the program of evaluating temperature fields is used time after time in the searching procedure. The temperature fields are not given new values after every repeating use. It is just to find out the values of temperature field relative to the BHTC which value is the endpoint of interval after cooling for definite time. So the values of temperature fields should be resumed to the original values after every repeating use. Then the error between computation values and objective values of temperature is evaluated using Eq. 5, and the searching direction and the convergent state can be ascertained according to the error. Only after the appropriate BHTC relative to certain objective values of temperature is found out, the temperature fields are refreshed and given new values.

3.3 Calculation of boundary heat transfer coefficient

The golden section method (GSM) is a technique for finding the extremum (minimum or maximum) of a strictly unimodal function by successively narrowing the range of interval inside which the extremum is known to exist [23]. GSM is one of the one-dimensional search methods for the unconstrained optimization, mainly used to evaluate the minimum or maximum value in the interval of unimodal distribution function. The function values relative to the different probe points are compared to narrow the interval in which the optimum value is included, and the approximative value of the function extremum will be achieved when the interval width is reduced to a prescriptive value.

The functional values of $E(x)$ are on the y-axis, and the x-axis is the boundary heat transfer coefficient. The values of $E(x)$ at the two end-points of interval $[a, b]$ have already been evaluated using the improved advance-retreat method. Since $E(a)$ is more than 0, and $E(b)$ is less than 0, it is clear that there is a value of BHTC which can minimize the functional values of $E(x)$ in the interval $[a, b]$, as shown in Fig. 3.

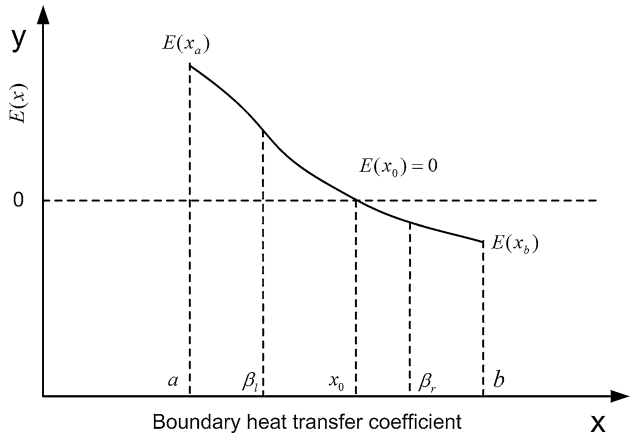

Fig. 3 Schematic diagram of golden section method

The next step is the process of narrowing the interval. A probe point β is in the interval $[a, b]$, and the functional values of $E(\beta)$ can be evaluated by the Eq. 5. If β is in the interval of from a to x_0, as β_l shown in Fig. 3, $E(\beta)$ is more than 0, then the new interval is $[\beta_l, b]$. If β is in the interval of from x_0 to b, as β_r shown in Fig. 3, $E(\beta)$ is less than 0, then the new interval is $[a, \beta_r]$. So, in either case, a new narrower search interval containing the function minimum can be attained.

Firstly, two probe points are selected in the interval $[a, b]$, suppose the left probe point is

$$\beta_{\mathrm{l}} = a + (1 - \tau)(b - a) \tag{6}$$

the right probe point is

$$\beta_{\mathrm{r}} = a + \tau(b - a) \tag{7}$$

where, τ is the solution of quadratic equation $\tau^2 + \tau - 1 = 0$.

Secondly, the values of left and right probe points are regarded as the BHTCs and used in the simulation of temperature fields. Then, the function values φ_{l} and φ_{r} relative to the left and right probe points are calculated using Eq. 5 according to the temperature values attained in the simulation.

$$\varphi_{\mathrm{l}} = E(\beta_{\mathrm{l}}), \quad \varphi_{\mathrm{r}} = E(\beta_{\mathrm{r}}) \tag{8}$$

Thirdly, according to the characteristics of unimodal distribution function, if $\varphi_{\mathrm{l}} < \varphi_{\mathrm{r}}$, there is not minimum value in the interval $[\beta_{\mathrm{r}}, b]$, the interval $[\beta_{\mathrm{r}}, b]$ can be neglected. Let $a' = a$ and $b' = \beta_r$, the new interval $[a', b']$ is $[a, \beta_{\mathrm{r}}]$. If $\varphi_{\mathrm{l}} > \varphi_r$, there is not minimum value in the interval $[a, \beta_{\mathrm{l}}]$, the interval $[a, \beta_{\mathrm{l}}]$ can be neglected. Let $a' = \beta_l$ and $b' = b$, the new interval $[a', b']$ is $[\beta_{\mathrm{l}}, b]$. The new probe points are selected using Eqs. 6 and 7 in the new interval $[a', b']$,

$$\begin{aligned} \beta_l &= a' + (1 - \tau)(b' - a') \\ \beta_r &= a' + \tau(b' - a') \end{aligned} \tag{9}$$

These steps are repeated until the difference between the upper and lower limits of interval reaches to the satisfied value. In the GSM, one of the new probe points is just the left or right probe point of old interval. That is to say, if τ values are the solutions of quadratic equation $\tau^2 + \tau - 1 = 0$, only one probe point and its function value need to be calculated in every iterative calculation except the first iterative calculation. So the calculation time of temperature field can be decreased largely, and the time of optimization also can be reduced largely.

The flow chart of gold section method is shown in Fig. 4.

The computation algorithm of GSM shows that, the length of interval is $\tau^{n-1}(b - a)$ after n times iterative evaluations. $b - a$ is the length of initial interval, which value is equal to the initial searching step size α_{s} of the improved advance-retreat method. So the iterative times of GSM depend on the initial searching step size α_{s} of the improved advance-retreat method.

3.4 Algorithm verification of calculating BHTC

In order to verify the feasibility and accuracy of algorithm used to calculate the BHTC, some BHTCs are assumed to depend on the surface temperature and used to analysis the cooling process of sample, the temperature curves at the certain positions of sample can be attained by using the FEM software package - MARC. In the evaluation, the assumed temperature-dependent BHTCs are shown in Fig. 5, and the thermal physical parameters of H13 steel are shown in Table 1. In the simulation of temperature field, the sample is H13 steel with the size of φ30 mm × 30 mm, and uniformly heated at 700 °C. The bottom surface of sample is cooled in 27 °C water. The FEM model includes 400 elements and 441 nodes. The circumference of sample is adiabatic except the bottom surface of sample. The cooling curves at the positions of 0, 3, 15, 30 and 60 mm away from the bottom surface of sample are shown in Fig. 5.

Then, the BHTCs are calculated using the inverse heat conduction analysis software according to the temperature–time curves. The initial searching step size 5 W/(m^2 °C) is adopted to search the interval using the improved advance-retreat method. The iteration condition used to optimize the interval size in the GSM is that, the interval size is more than 0.1 W/(m^2 °C) or the maximum difference between the measured and calculated temperature is more than 0.01 °C. The convergence criteria in the calculation of temperature is that the maximum temperature difference between the current iteration and next iteration is less than 0.00001 °C. By using the improved advance-retreat method, the number of iterations for each interval is generally in the range of 3–15 times (the number of iterations is 19 times for the first interval). In the process of optimizing the interval size, the number of iterations is in the range of 3–6 times by using golden section method, which are shown in Fig. 6.

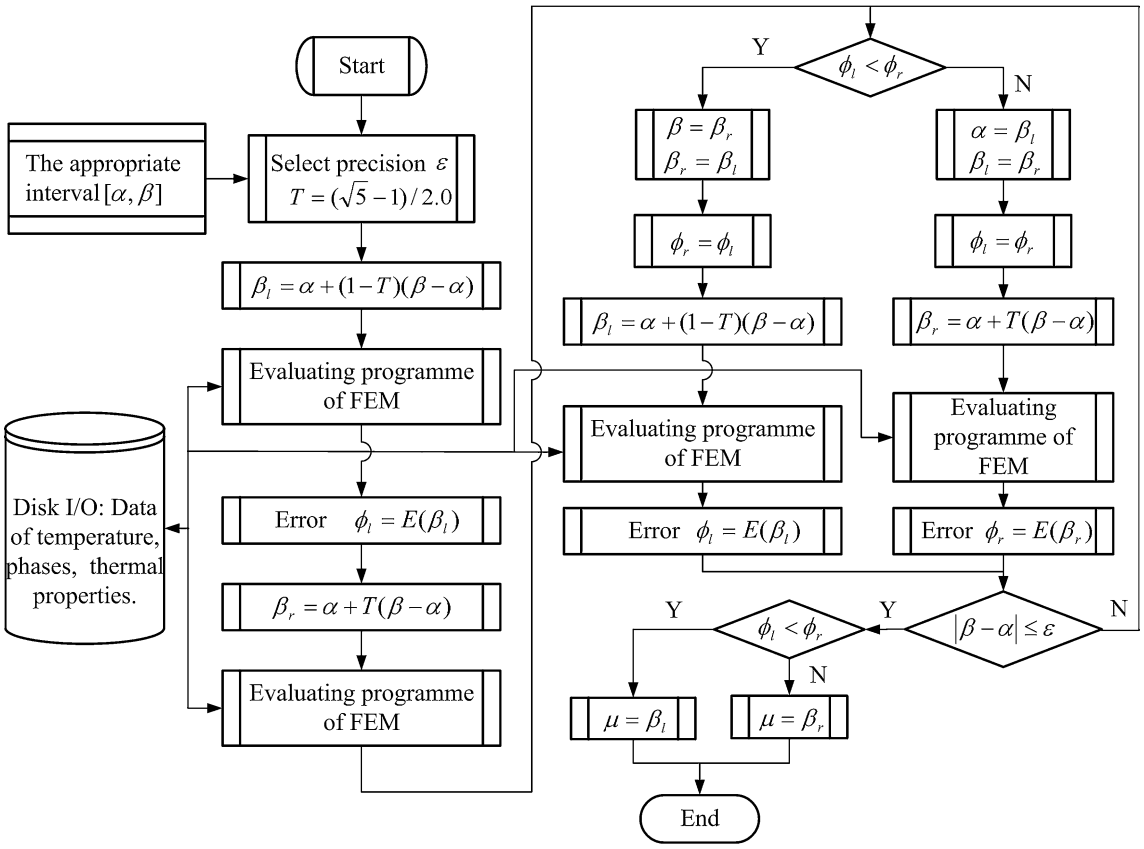

Fig. 4 Flow chart of gold section method

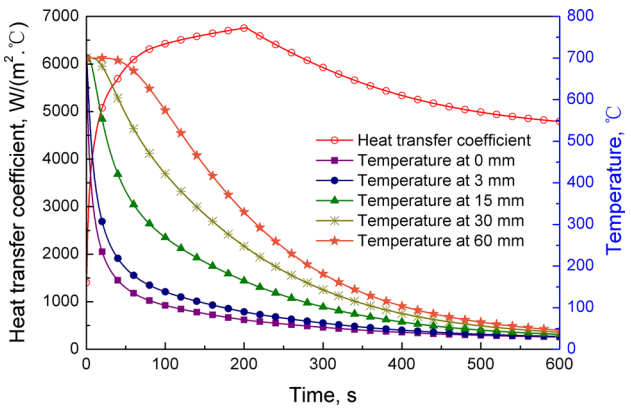

Fig. 5 Temperature and heat transfer coefficient versus time curves

The calculated data of BHTC is shown in Fig. 7. The accuracy of algorithm can be verified by comparing the difference between the assumed and calculated BHTCs. The data of BHTC in Fig. 7 show that, the calculated data of BHTCs are well consistent with the assumed data of BHTCs, the computation accuracy and reliability of the inverse heat conduction analysis software is well.

4 Solution of BHTC between the cooling water and die

4.1 Measurement equipment

The BHTC between the cooling water and die is an important parameter in the hot stamping process. The test system shown in Fig. 8 is designed to record the cooling curves of sample and calculate the BHTC according to the cooling curves. This system mainly includes the sample of H13 steel, thermal insulation material, thermocouples, high speed USB data collection device, inverse heat conduction analysis software, cooling water spray system (which is used to spray water to the bottom surface of sample) and so on. The sample material is H13 steel, which chemical compositions are listed in Table 2. The thermal physical parameters of H13 steel, such as linear expansion coefficient, density, specific heat capacity and thermal conductivity, are shown in Table 1. Steel plate around the bottom surface of sample is used to protect the thermal insulation material from water. The thermal insulation material is the ceramic fiber paper made from high purity alumino-silicate fiber through a fiber washing process, its thermal conductivity is

Table 1 Thermal physical parameters of H13 steel

Temperature	25 °C	300 °C	500 °C	700 °C
Linear expansion/ C^{-1}	1.1×10^{-5}	1.17×10^{-5}	1.23×10^{-5}	1.31×10^{-5}
Density/Kg/m^3	7.80×10^3	7.71×10^3	7.64×10^3	7.58×10^3
Specific heat capacity/J/(kg °C)	460	511	548	595
Thermal conductivity/W/(m °C)	25.0	26.9	28.6	30.4

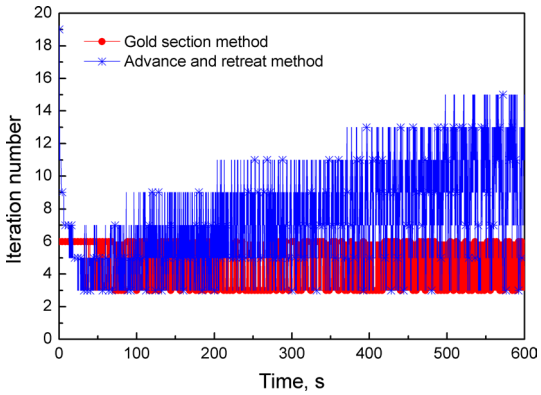

Fig. 6 Iteration numbers of advance-retreat method and gold section method

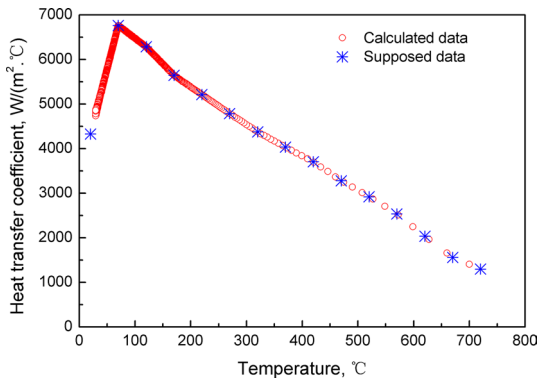

Fig. 7 Comparison of calculated and assumed BHTCs

0.02–0.075 W/(m °C). The thermal insulation material covers the surfaces of sample expect the bottom surface. Heat transfer between the cooling water and sample only happens on the bottom surface of sample. In order to simplify the finite element model of simulation and make it easy to calculate the BHTC, assume that the heat transfer of sample is in the state of one-dimensional conduction due to the small thermal conductivity of thermal insulation material.

The flow chart of test is shown in Fig. 8. The temperature variation of sample is translated into the voltage signals by the NiCr–NiSi thermocouples, then the voltage signals are recorded, filtered, amplified and converted (analog to digital, A/D) by the high speed USB data collection device, and transformed into the corresponding temperatures by the data collection software. The NiCr–NiSi thermocouple is with the diameter of 2 mm and the length of 100 mm, the measurement tolerance is ±1.0 °C in the temperature range from −50 to 1200 °C, the response time is 0.02 s. The speed of A/D converter of the high speed USB data collection device is 0.1 s.

The flow chart of calculating the BHTC is shown in Fig. 9. The improved advance-retreat method, GSM and FEM method are used to calculate the BHTC according to the temperature data recorded by the test system.

4.2 Acquisition of temperature–time curves

In order to reduce the experimental error and uncertainty, two types of samples are designed. The dimensions of samples are shown in Fig. 10. The blind hole with the diameter of 2.5 mm is used to insert the thermocouple. The difference of these samples is shown by the distance between the bottom of the blind hole and the bottom surface of sample. The distance of some samples is 1 mm, and that of the other samples is 2 mm.

The surfaces of sample expect the bottom surface are covered by the thermal insulation material. Heat transfer between the cooling water and sample only happens on the bottom surface of sample. A piece of steel plate is used in the test, which is with the thickness of 1.6 mm, the diameter of 80 mm and a hole of diameter $\varphi 30^{-0.1}_{-0.2}$ mm in the center. This steel plate is fixed on the bottom end of sample to prevent the cooling water from dipping into the thermal insulation material and affecting the thermal insulation characteristic of thermal insulation material. The assembly relationship of the sample and steel plate is shown in Fig. 8.

The program-control chamber electric furnace SX2-4-10G is used to heat the sample. The temperature of furnace is set to 700 °C. The samples with the steel plate and the thermal insulation material are placed inside the furnace and heated for about 60 min to ensure the temperature uniformity distributed in the samples. A steel block with the diameter of 80 mm and the height of 50 mm is also heated in the furnace. 99.999 % nitrogen is used to protect the samples and the steel block from oxidation during heating. First, the steel block is taken out and placed on the thermal insulation material. Then, the sample is taken out and placed on the steel block, and the thermocouple is quickly inserted to the hole of sample. When the temperature

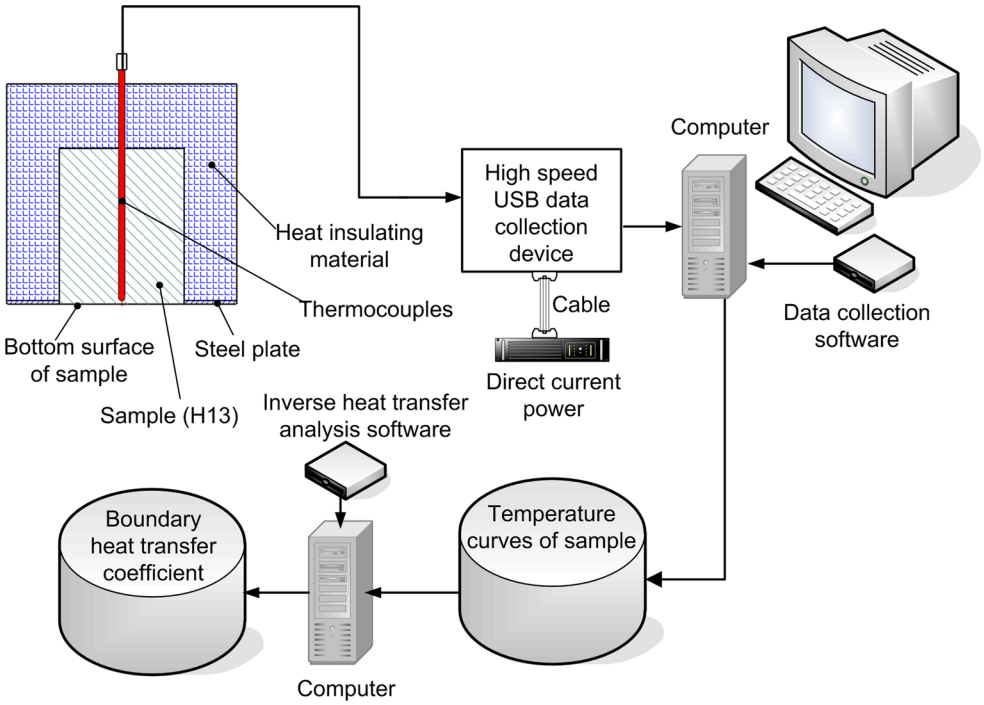

Fig. 8 Test system of the BHTC between the cooling water and die

Table 2 Chemical compositions of H13 steel (unit: wt%)

Composition	C	Si	Mn	P	S	Cr	Mo	V	Cu	Ni	W
wt%	0.38	0.96	0.27	0.017	0.007	4.75	1.15	0.9	0.1	0.12	0.37

shown in the computer keeps steadily, the sample is rapidly moved to the test equipment and cooled by the spraying water. In the test, the temperature of cooling water is about 20 °C, the pressure of water is about 0.35 Mpa, the water speed is about 1.6 m/s, the diameter of cooling water outlet is about 20 mm, the distance between the outlet of cooling water and the cooling end of sample is about 50 mm. Some temperature–time curves recorded by the high speed USB data collection device are shown in Fig. 11.

The legend number '1 mm–678.36 °C' in Fig. 11 means the temperature–time curve is measured in the sample (a) shown in Fig. 11, and the initial temperature of sample is 678.36 °C. The meaning of other legend numbers in Fig. 11 is similar to that.

4.3 Calculation of boundary heat transfer coefficient

In order to simplify FEM model of sample, the hole used to insert the thermocouple and the heat transfer between the steel plate and sample are not considered in the FEM model, the FEM model of sample is shown in Fig. 12. There are 400 elements and 441 nodes in the model. In the region close to the bottom surface, the mesh size along the axis of sample is 1 mm. In the region close to the top surface, the mesh size along the axis of sample is 2 mm. In the other region, the mesh size along the axis of sample is 1.5 mm. The two black solid points shown in Fig. 12 are the end position of thermocouple in the experiment. The distance of the two points away from the bottom surface of sample is respectively 1 mm and 2 mm. Two types of boundary conditions are needed to set in the FEM model. One is an unknown heat transfer coefficient between the cooling water and the bottom surface of sample, the other is the certain heat transfer coefficient around the other surface of sample.

In the process of searching the interval, the iteration number at t = 131.6 s is 14 times by using the improved advance-retreat method, the iteration error and interval variation are shown in Fig. 13a, b. The left point of interval can let $E(x) > 0$ (as shown in Eq. 4; Fig. 3), and the right point of interval can let $E(x) < 0$ when the iteration number reaches to 6. It means that there is the value minimizing the error in the interval. Then the size of interval is reduced using the advance and retreat method, and the size of interval reaches to 1.25 as the iteration number is 14. In the process of minimizing the interval size, the iterative number at t = 131.6 s is 6 times by using the golden section method, the iterative error and interval variation are

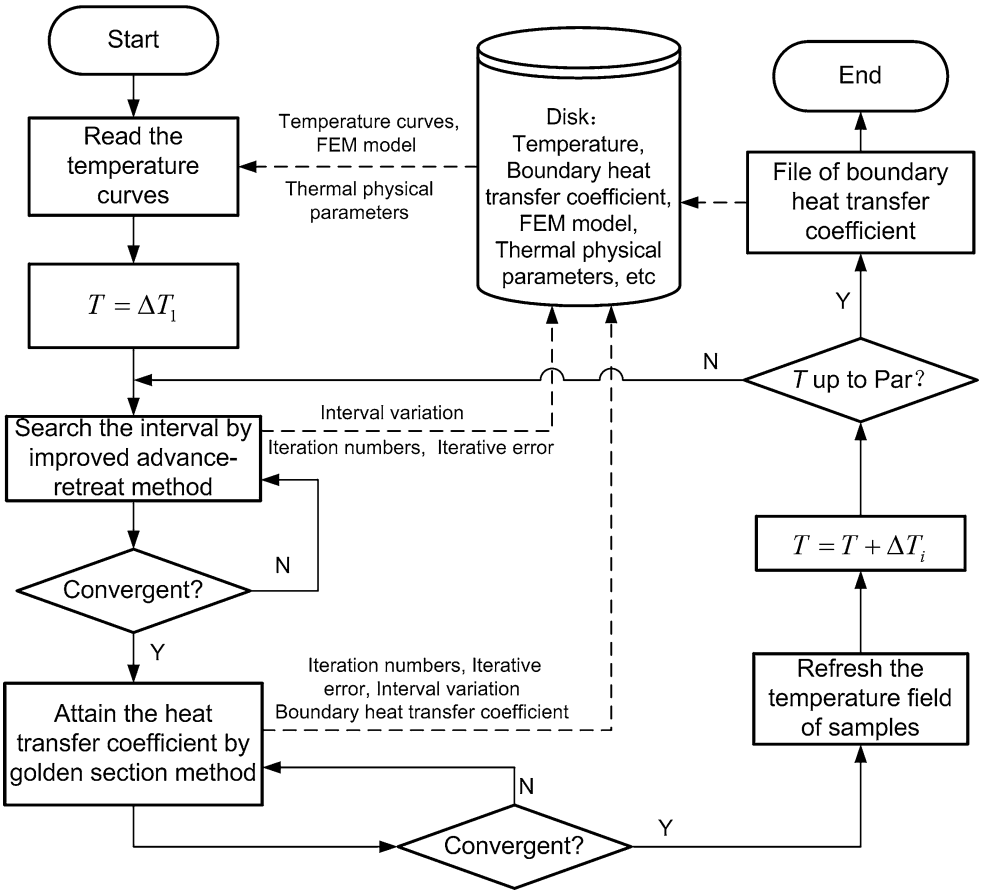

Fig. 9 Flow chart of calculating heat transfer coefficient

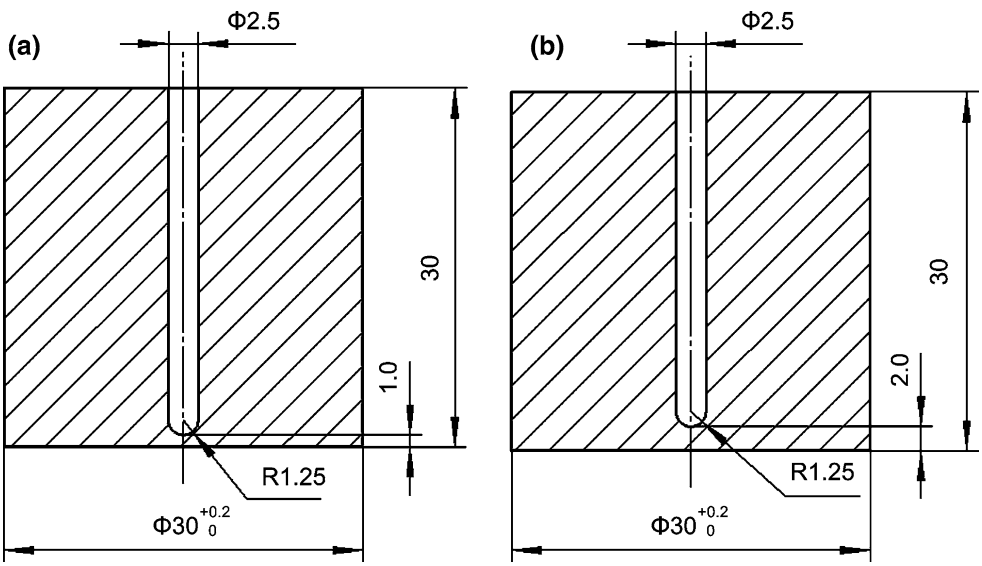

Fig. 10 Dimensions of tool samples (unit: mm)

shown in Fig. 14a, b. The size of interval reaches to 0.01 as the iteration number is 6. It means that the BHTC minimizing the difference between the measured temperature and calculated temperature at t = 131.6 s is in this interval. The error of BHTC will be less than 0.01 W/(m^2 °C), and it can meet the requirement of the convergence criteria ($|E(\alpha)| < 0.00001$ °C).

According to the temperature curves (678.36, 693.02, 688.21 and 693.98 °C) shown in Fig. 11, four groups of BHTCs are attained by the inverse heat conduction analysis

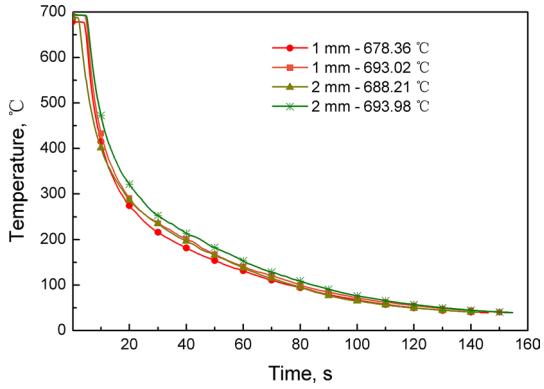

Fig. 11 Temperature-time curves recorded in the test

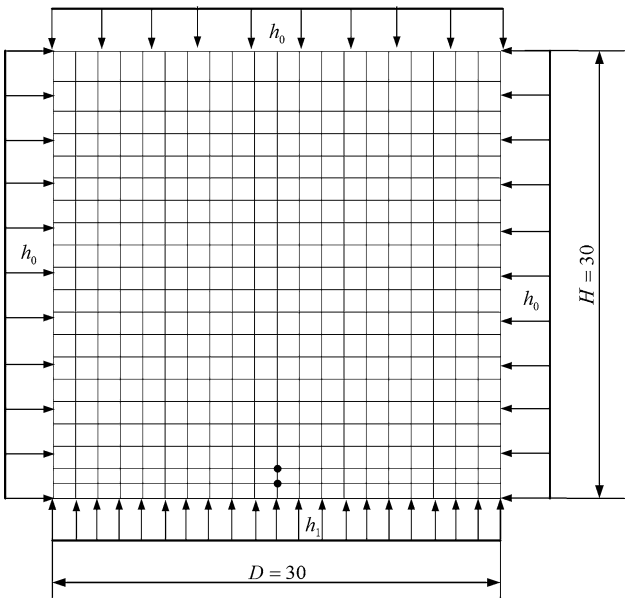

Fig. 12 Finite element model of sample

software. The BHTCs between the cooling water and sample are calculated by using the improved advance-retreat method, GSM and finite element method, which are shown in Fig. 15. The distribution trend of four groups of data is very similar, and the curve fitting can be done according to these data, the fitting curve is shown in Fig. 15.

The fitting data of BHTCs shown in Fig. 15 are used to simulate the cooling process of 'sample a' and 'sample b' shown in Fig. 10. The calculated data and measured data of temperature, the difference between the calculated and measured data are shown in Fig. 16. It shows the calculated data of temperature are consistent with those of measured. The accuracy and effectiveness of the method developed to evaluate the inverse heat conduction problem in the paper are well.

In the process of experiments, the significant boiling happens on the boundary surface of sample and water. Boiling is the rapid vaporization of a liquid, which occurs when a liquid is heated to its boiling point, the temperature at which the vapor pressure of the liquid is equal to the pressure exerted on the liquid by the surrounding environmental pressure. Boiling occurs in three characteristic stages, which are nucleate, transition and film boiling stage. These stages generally take place from low to high heating surface temperatures, respectively.

Some researchers have attained the BHTCs between the steel and static-state water without pressure (pool boiling at 1 atm), as curves 1, 2, 3, 4 and 5 shown in Fig. 17 [24–27]. These BHTC curves show that, there are four characteristic stages in these curves for the pool cooling, which are natural convection, nucleate boiling, transition boiling and film boiling, as shown in Fig. 18. It is the film boiling stage when the surface temperature of sample is more than 400 °C, and the BHTC is smaller. In this stage, on the surface of sample heating water is significantly hotter

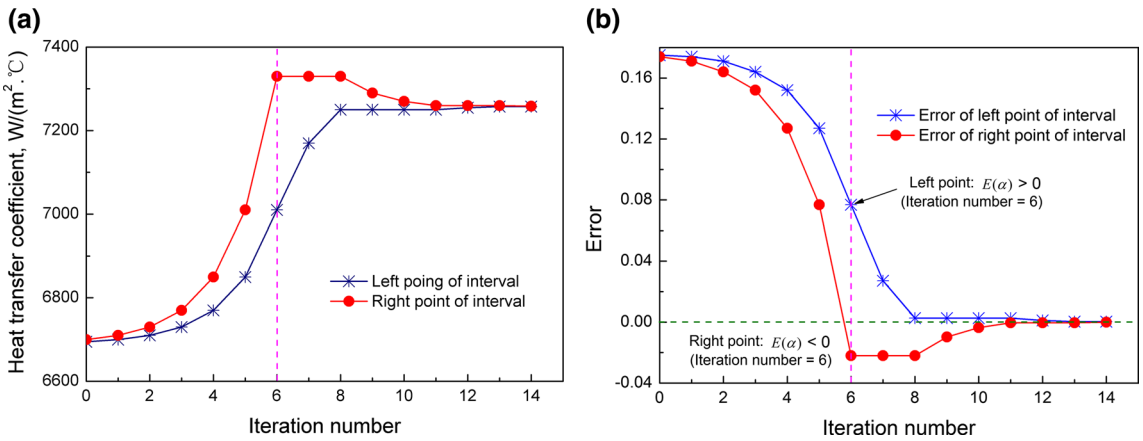

Fig. 13 Iteration error and interval variation using the improved advance-retreat method (t = 131.6 s). **a** Interval variation of heat transfer coefficient. **b** Iteration error

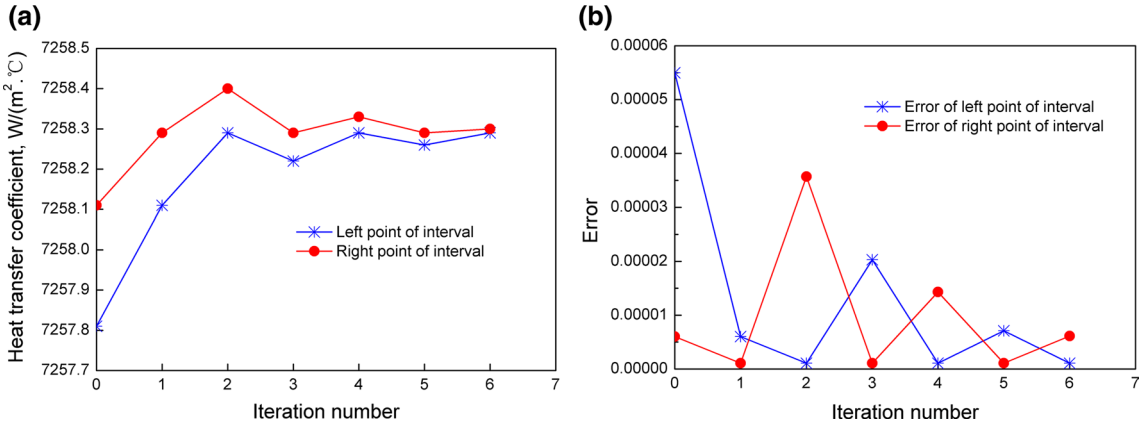

Fig. 14 Iteration error and interval variation using the golden section method (t = 131.6 s). **a** Interval variation of heat transfer coefficient. **b** Iteration error

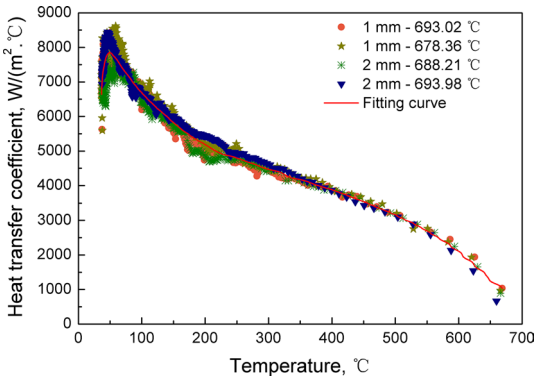

Fig. 15 BHTCs between hot sample and cooling water (20 °C)

than water, film boiling will occur on the boundary surface of sample and water. A thin layer of vapor, which has low thermal conductivity, insulates the surface of heat transfer.

The transition boiling is probably the least studied region of the boiling curve. In this region (about 250–400 °C shown in Fig. 17), the liquid periodically contacts the heating surface, and then produces large amounts of vapor to force the liquid away from the surface. The combined result leads to an unstable vapor film or blanket. As the film collapses, the liquid is allowed to contact the heating surface again. The BHTC in this stage is larger than that in the film boiling stage [28].

The nucleate boiling is in the range from 100 to 250 °C, as shown in Fig. 17. The isolated bubbles form at nucleation sites and separate from the boundary surface. This separation induces considerable fluid mixing near the boundary surface, substantially increasing the convective heat transfer coefficient and the heat flux. In this stage, most of the heat transfer is through direct transfer from the surface of sample to water in motion at the boundary surface and not through the vapor bubbles rising from the boundary

Fig. 16 Difference between the calculated and measured results of temperature

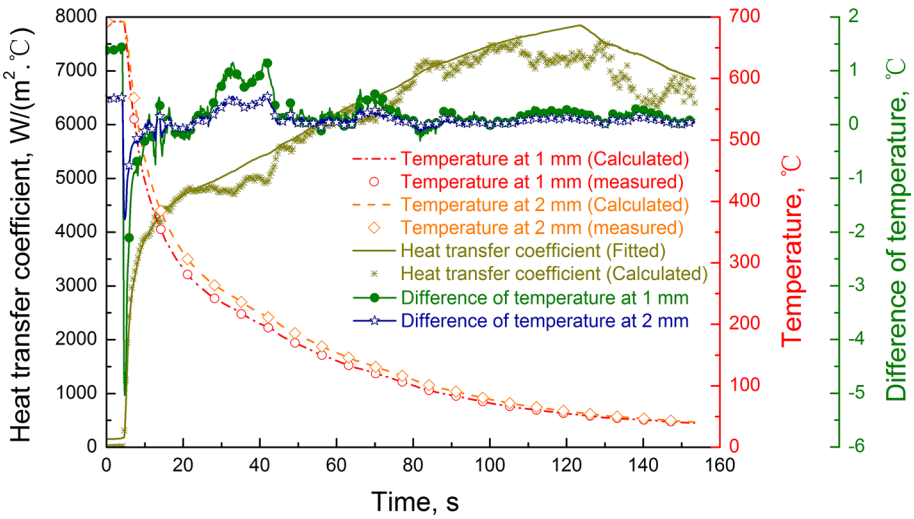

surface [29]. The BHTC in this stage is similar to that in the transition boiling stage.

In the paper, the cooling agent is the flowing water with the low-pressure (20 °C, 0.35 MPa, and 1.6 m/s), it is different from the static water without pressure in the references [24–27]. At the stage of film boiling, a film of vapor forms on the surface due to the significantly high surface temperature, it is very difficult for the low-pressure flowing water to destroy the water vapor and contact the sample surface with high temperature. So the BHTC calculated in the paper is similar to that attained using the static water without pressure by some researchers. Since this vapor film is much less capable of carrying heat away from the surface, the BHTC is small, and the heat flux from the surface of sample to water is slow.

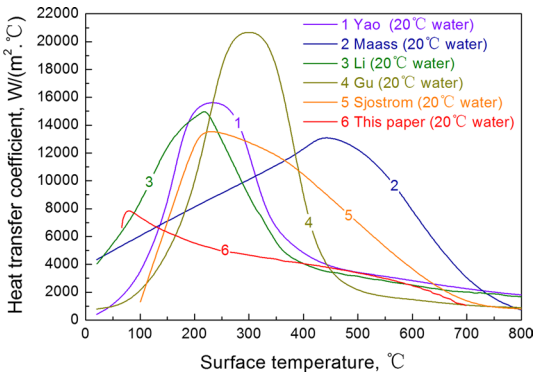

Fig. 17 BHTCs attained by some researchers

At the stages of nucleate and transition boiling, the BHTCs are different from that attained by other researchers. This can be explained with Newton's law of cooling,

$$q = H(T_w - T_c) \tag{10}$$

where, q represents the heat flux, H represents the BHTC, T_w represents the surface temperature of sample, and T_c represents the temperature of cooling water close to the sample. In the references [24–27], the temperature of vapor film or the temperature of cooling water close to the sample is neglected as it is difficult to be measured by sensor or calculated using the couple analysis method by software. In the calculation of BHTC, the initial temperature of water is regarded as T_c. If T_c rises significantly due to the vapor film, H will increase for fixed q and T_c.

Although the BHTC attained in this paper is smaller than that attained by other researchers in the temperature range from 100 to 400 °C, the heat exchange between the sample and the flowing water is much larger than that of sample in the static water. The reason is that, except the stage of film boiling, the heat exchange between the sample and the flowing water is similar to the nucleate boiling or natural convention shown in Fig. 18a, b, the temperature T_c in Eq. 10 is close to the temperature of flowing water (20 °C) due to the pressure and flowing of water. The heat exchange between the sample and the static is the nucleate and transition boiling in the temperature range from 100 to 400 °C, the temperature T_c in Eq. 10 is close to the boundary temperature of sample T_w, the value of $T_w - T_c$ is very small.

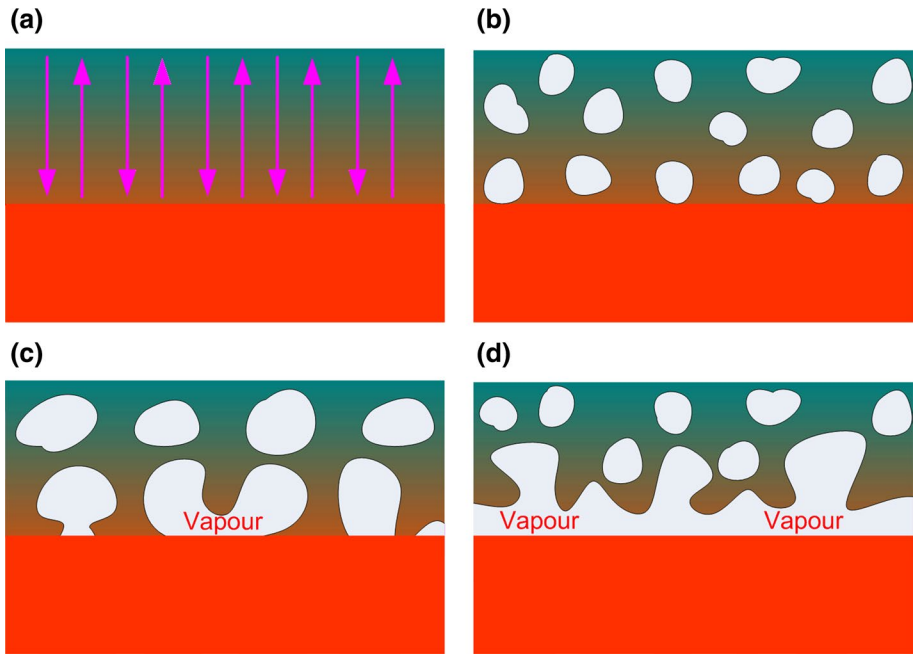

Fig. 18 Four stages of pool boiling. **a** Natural convection, **b** nucleate boiling, **c** transition boiling, **d** film boiling

5 Conclusions

The BHTC between the cooling water and sample is researched in the paper. NiCr–NiSi thermocouples are used to measure the temperature of sample. The high speed USB data collection device is used to acquisite the electrical signal from the thermocouples. The inverse heat conduction analysis software is used to calculate the BHTC according to the temperature–time curves. The research results show that:

1. The surface temperature of sample has a significant effect on the BHTC. The BHTC increases as the surface temperature of sample reduces, and the variation is nonlinear. The convergence of the method given in the paper is well.
2. At the stage of film boiling, a film of vapor forms on the surface due to the significantly high surface temperature, it is very difficult for the low-pressure flowing water to destroy the water vapor and contact the sample surface with high temperature.
3. When water sprays on the boundary surface of sample, the BHTCs at the stages of nucleate and transition boiling are different from that attained in the static water.
4. Although the BHTC in the flowing water is smaller than the BHTC in the static water in the temperature range from 100 to 400 °C, the heat exchange between the sample and the flowing water is much larger than that of sample in the static water.

Acknowledgments This work was financially supported by the National Natural Science Foundation of China (51175302), Taishan Scholars Project of Shandong (TS20110828), the Program for New Century Excellent Talents in University (NCET-12-0342), the Science and Technology Development Program of Shandong and Huangdao (2014GGX103024, 20140132) and Scientific Research Foundation of Shandong University of Science and Technology for Recruited Talents (2013RCJJ002 and 2013RCJJ005).

References

1. Gu JF, Pan JS, Hu MJ (1998) Inverse heat conduction analysis of synthetical surface heat transfer coefficient during quenching process. J Shanghai Jiaotong Univ 32:18–22
2. Park HM, Chung OY, Lee JH (1999) On the solution of inverse heat transfer problem using the Karhunen–Loeve Galerkin method. Heat Mass Transf 42:127–142
3. Taler J, Zima W (1999) Solution of inverse heat conduction problems using control volume approach. Heat Mass Transf 42:1123–1140
4. Chantasiriwan S (2000) Inverse determination of steady-state heat transfer coefficient. Heat Mass Transf 27:1155–1164
5. Chen NL, Pan JS, Liao B, Gao CY (2002) Measurement and calculation of the heat transfer coefficient of dynamic quenchant. Hot Work Technol 3:6–7
6. Li HP, Zhao GQ, Niu ST et al (2006) Inverse heat conduction analysis of quenching process using finite-element and optimization method. Finite Elem Anal Des 42:1087–1096
7. Lesnic D, Elliott L, Ingham DB (1996) Application of the boundary element method to inverse heat conduction problems. Heat Mass Transf 39:1503–1517
8. Lesnic D, Elliott L (1999) The decomposition approach to inverse heat conduction. J Math Anal Appl 232:82–98
9. Kim S, Kim MC, Kim KY (2002) An integral approach to the inverse estimation of temperature-dependent thermal conductivity without internal measurements. Int Commun Heat Mass Transf 29:107–113
10. Shen SY (1999) A numerical study of inverse heat conduction problems. Comp Math Appl 38:173–188
11. Tseng AA, Chen TC, Zhao FZ (1995) Direct sensitivity coefficient method for solving two-dimensional inverse heat conduction problems by finite element scheme. Numer Heat Transf B 27:291–307
12. Merklein M, Lechler J, Stoehr T (2009) Investigations on the thermal behavior of ultra high strength boron manganese steels within hot stamping. Int J Mater Form 2:259–262
13. Karbasian H, Tekkaya AE (2010) A review on hot stamping. J Mater Process Technol 210:2103–2118
14. Hein P, Wilsius J (2008) Status and Innovation trends in hot stamping of USIBOR 1500P. Steel Res Int 79:85–91
15. Maikranz-Valentin M, Weidig U, Schoof U et al (2008) Components with optimised properties due to advanced thermomechanical process strategies in hot sheet metal forming. Steel Res Int 79:92–97
16. Caron E, Daun KJ, Wells MA (2014) Experimental heat transfer coefficient measurements during hot forming die quenching of boron steel at high temperatures. Int J Heat Mass Transf 71:396–404
17. Bosetti P, Bruschi S, Stoehr T et al (2010) Inter laboratory comparison for heat transfer coefficient identification in hot stamping of high strength steels. Int J Mater Form S1:817–820
18. Abdulhay B, Bourouga B, Dessain C et al (2009) Experimental study of heat transfer in hot stamping process. Int J Mater Form 2:255–257
19. Abdulhay B, Bourouga B, Dessain C (2012) Thermal contact resistance estimation: influence of the pressure contact and the coating layer during a hot forming process. Int J Mater Form 5:183–197
20. Li HP, He LF, Zhao GQ (2013) Research on the surface heat transfer coefficient depending on surface pressure of boron steel B1500HS. Chin J Mech Eng 49:77–83
21. Zhang ZQ, Li XS, Zhao Y et al (2014) Heat transfer in hot stamping of high-strength boron steel sheets. Metall Mater Trans B 45:1192–1195
22. Kong XQ (1998) The application of finite element method in the heat transfer. Science Press, Beijing
23. Press WH, Teukolsky SA, Vetterling WT, Flannery BP (2007) Section 10.2 golden section search in one dimension, numerical recipes: the art of scientific computing, 3rd edn. Cambridge University Press, New York
24. Gu JF, Pan JS, Hu MJ (1998) Computer measurement and calculation on heat transfer coefficients of quenchants. Hot Work Technol 5:13–14
25. Sjostrom S (1985) Interactions and constitutive models for calculating quench stresses in steels. Mater Sci Technol 1:823–829
26. Yao X, Gu JF, Hu MJ (2003) 3D temperature and microstructure modeling of large-scale P20 steel mould quenching in different process. Heat Treat Met 28:33–37
27. Li HP, Zhao GQ, Niu ST, Luan YG (2006) Acquisition of cooling curve during quenching process and research on evaluating method of heat transfer coefficient. Heat Treat Met 31:29–32
28. Witte LC, Lienhard IH (1982) On the existence of two transition boiling curves. Int J Heat Mass Transf 25:771–779
29. Hohl R, Auracher H, Blum J, Marquardt W (1996) Pool boiling heat transfer experiments with controlled wall temperature transients. In: 2nd European thermal science and 14th UIT national heat transfer conference, Rome, pp 1647–1652